

535-12
150611
P-10

AN X-RAY SCATTER APPROACH FOR NON-DESTRUCTIVE CHEMICAL
ANALYSIS OF LOW ATOMIC NUMBERED ELEMENTS

H. Richard Ross
Sverdrup Technology, Inc.
NASA John C. Stennis Space Center, MS 39529

ABSTRACT

A non-destructive x-ray scatter (XRS) approach has been developed, along with a rapid atomic scatter algorithm for the detection and analysis of low atomic-numbered elements in solids, powders and liquids. The present method of energy dispersive x-ray fluorescence spectroscopy (EDXRF) makes the analysis of light elements (i.e. less than sodium; < 11) extremely difficult. Detection and measurement become progressively worse as atomic numbers become smaller, due to a competing process called "Auger Emission", which reduces fluorescent intensity, coupled with the high mass absorption coefficients exhibited by low energy x-rays, the detection and determination of low atomic-numbered elements by x-ray spectrometry is limited. However, an indirect approach based on the intensity ratio of Compton and Rayleigh scatter has been used to define light element components in alloys, plastics and other materials. This XRS technique provides qualitative and quantitative information about the overall constituents of a variety of samples.

INTRODUCTION

Qualitative and quantitative determination of the elemental content of a wide variety of samples is vital in many fields of science, technology, and industry. Energy dispersive x-ray fluorescence spectroscopy (EDXRF) is the best known rapid, sensitive, and non-destructive technique for identifying unknown elements in solids, powders, and liquids. Samples that contain high levels of light elements are not amenable to EDXRF detection. Therefore, this method is not capable of providing reliable estimates of elemental concentrations for low atomic number based materials. Corrosion and contamination products are often compounds containing low atomic numbered elements (i.e. oxides, carbonates, nitrates and hydrates), which are costly to detect and time consuming. EDXRF analysis reveals only heavy elements, therefore failing to represent the bulk composition of the contaminants.

Recently, a non-destructive x-ray scatter (XRS) approach has been developed at the NASA John C. Stennis Space Center. XRS can provide qualitative and quantitative information about the overall constituents of a variety of samples. The experimental results presented in this paper, show the versatility and importance of XRS in analyzing complex low atomic numbered materials.

EXPERIMENTAL CONDITIONS

System

A schematic of the Spectrace Corporation (Mountain View, California) EDXRF system geometry and components is shown in Figure 1. Developments in the system's hardware, the technique itself, the theory, and the performance characteristics are mentioned in the literature [1-2].

Operating Parameters

A complete list of the experimental conditions is provided in Table 1. The spectrometer used in this study was a Spectrace 440 EDXRF Analyzer equipped with a molybdenum target x-ray tube, which operates at 50W of power. All scatter measurements were made with a 0.0625 inch diameter collimator and were taken for 90 seconds per sample. In all tests a minimum of 20,000 counts were acquired for each sample, and the counting procedure was repeated four times. The percent RSD was less than 3%.

Spectrometer	Spectrace 440 Energy Dispersive Analyzer
X-ray Tube	Molybdenum Anode Target
Excitation Conditions	50 kV, 0.1 mA, Direct Excitation
Count Cycle	90 Seconds Real Time
Dead Time	48%
Collimator Diameter	0.0625 inches
Pulse Processor	Time Constant 12.5 μ s
X-ray Path	Air

Table 1: Experimental Conditions

THEORY

The presence of Compton (incoherent) and Rayleigh (coherent) scatter peaks are routinely observed in x-ray fluorescence spectra and are considered a nuisance. In fact, scatter is a major source of background which limits analytical sensitivity and may cause spectral interference [3]. Figure 2 displays the output of a Rhodium x-ray tube operated at 30kV scattered from a polyester plug. The intense continuum output of the tube scattered from the polyester plug is apparent. Rhodium characteristic lines appear in the form of the Compton and Rayleigh scatter peaks. Rayleigh scatter is indicated by characteristic x-rays from the anode of the x-ray tube scattered to the detector without a change in energy, and Compton scatter is characterized by an energy loss that occurs in the sample.

When x-ray photons strike a collection of atoms, the photons may interact with electrons of the target atoms resulting in the scatter of the x-ray photons as illustrated in Figure 3. The scatter of the x-ray photons is caused mainly by outer, weakly-held electrons. If the collisions are elastic, scatter occurs with no loss of photon energy and is known as Rayleigh scatter. If the photon loses energy, causing the ejection of an electron, the scatter is inelastic and results in Compton scatter [1,4].

The energy loss associated with Compton scatter results in a predictable change in wavelength of the radiation given by Eq. 1:

$$\Delta\lambda = 0.243 (1 - \cos \phi), \quad (1)$$

because most x-ray spectrometers have a primary beam-sample-detector angle of 90° , $\phi = 90$ and $\cos \phi = 0$. Therefore, the Compton wavelength shift, which is shown in Eq. 2, is known as the Compton Wavelength;

$$\Delta\lambda = 0.0243. \quad (2)$$

In energy dispersive systems the Compton shift may be more effectively expressed as shown in Eq. 3:

$$E = 12.396 \div 0.0243, \text{ when } \Delta E = 0.510, \quad (3)$$

where E is in kV and λ is in Angstroms. For example, a molybdenum Compton scatter signal has an observed energy peak at 16.968 kV, as shown in Eq. 4:

$$17.478 \text{ kV} - 0.510 \text{ kV} = 16.968 \text{ kV}. \quad (4)$$

There are two important points to recognize concerning the application of x-ray scatter intensities for

measuring light element contributions of a sample; a larger observed Compton scatter is seen from samples with low atomic number matrices because there is less absorption by the sample; and the ratio of Compton-to-Rayleigh scatter intensity increases as the average atomic number of the sample decreases, as shown in Figure 4 [6]. Therefore, x-ray fluorescence scatter can provide qualitative and quantitative information about a variety of samples. Most significantly, the x-ray scatter spectrum signal yields information about the overall sample constituents and exploits the sensitivity of scatter parameters by combining the estimates of light elements with EDXRF measurement of the remaining elements. The x-ray scatter system helps discriminate light elements in metal alloys, and also determines the percentage of each component by using the XRS signal to compute the Atomic Scatter Factor (ASF) as shown in Eq. 5:

$$ASF = \sum_{i=1}^{i=N} (w_i)(Z_i). \quad (5)$$

The ASF includes the following properties: the ASF of an element is the same as the atomic (Z) number of the element, and the ASF of a compound or a mixture of elements is the mass sum fraction(s) of element i(w_i) multiplied by the Z number of element i, where N=number of elements. The XRS algorithms contain their own calibration curves, relating the Compton/Rayleigh scatter signal ratio to atomic number and for calculating a given chemical formula.

EXPERIMENTAL RESULTS

Corrosion and Contamination

Corrosion and contamination often represent critical problems for government agencies as well as industry. XRS analysis can effectively solve these problems, since compounds containing light elements are often associated with corrosion and contamination products. EDXRF analysis of contaminant spots on a low-alloy steel housing reveals iron as the only detectable heavy element. XRS analysis indicate that these spots have an ASF of 20.6. This information was input into the XRS program which generated the formula Fe₂O₃ as the only possibility, thus revealing the contamination to be simple rust spots and not a more complex contaminant.

The XRS identification algorithm is based upon comparison of net intensities of the selected elements in the unknown sample with those of the known reference samples. First a "Library" of references must be created using a set of known samples as shown in Table 2.

Substance	Atomic Scatter Factor	C/R
Fe	26.0	0.58
Fe ₃ O ₄	21.0	0.89
Fe ₂ O ₃	20.6	1.18
FeCO ₃	16.5	1.65
FeN ₃ O ₉ · 9H ₂ O	10.1	3.71

Table 2: "Library" of Known References

After choosing the elements to be employed in the identification, each reference sample is measured long enough (usually 90-120 sec) to make the statistical counting error negligible. The net intensities of the selected elements (Z > 12) and the Compton-Rayleigh backscatter ratios are calculated and stored in the "Scatter Library" along with their standard deviations and a formula label of the reference sample.

After the library of references is complete, a measurement of the unknown sample can be performed. The net intensities (I_i) of the unknown sample are calculated and a statistic (t_s) is created for each of the possible K pairs, where K is the number of references in the library. The statistic (t_s) is shown in Eq. 6:

$$t_s = \sum_{i=1}^N \frac{(I_{ix} - I_{ik})^2}{\sigma^2(I_{ix}) + \sigma^2(I_{ik})}, \quad (6)$$

where I_x and I_k are the net intensities of the i^{th} element of the unknown and the k^{th} reference, respectively; σ_{I_x} and σ_{I_k} are the standard deviations of these intensities; and N is the number of intensities measured. The statistic (t_s) is a squared Euclidean distance coefficient (dxk), between the unknown sample and the k^{th} reference, weighted with the variances of measured intensities. During the actual identification, the program sequentially compares intensities of the unknown with those of the references, (See Figure 5 & 6) calculating for each pair (unknowns) its t_s value, and selecting the smallest of them. If the smallest t_s value is greater than 90% threshold, then the second smallest t_s value is also retrieved and names of both references are displayed along with the message "possible fit". However, both t_s 's must also be less than the 99.9% confidence level threshold, or the algorithm will determine that none of the references match the sample and will display "no match found".

Solvent Mixtures

The analysis of hydrocarbon components is of critical importance in the assessment of the integrity of clean systems used in the National Aeronautics and Space Administration (NASA) Space Shuttle Main Engine (SSME) Testing Program. These analyses are based on the removal of residues from hardware critical surfaces by means of flushing the surfaces with approved halogenated solvents. Infrared spectroscopy has been widely used in the detection of these impurities. However, there are limitations with this technique caused by the strong infrared absorbance band that are characteristic of these halogenated solvents. Consequently, when analyzed by infrared spectroscopy, the solvent bands are totally absorbing, which makes the detection of several hydrocarbons in the infrared spectral region impossible.

XRS spectroscopy has proven to be a significant improvement in the speed and accuracy of infrared measurements. This procedure is based on the application of hydrocarbons expressed as isopropyl alcohol (IPA) in chlorofluorocarbon (CFC) 113. Scatter rate ratios were obtained from the calibration mixtures and are tabulated in Table 3.

% CFC 113	% IPA	Molecular Wt.	% Hydrogen	C/R
100	0	187.37	0.0	0.6673
80	20	161.92	0.51	0.8584
60	40	136.47	1.2	1.1835
50	50	123.74	1.9	1.2740
40	60	111.01	2.5	1.5656
20	80	85.55	5.3	2.6341
0	100	60.10	13.42	5.1118

Table 3: Calibration data and results for hydrogen x-ray scatter analysis of IPA in CFC 113.

The calibration curve for hydrogen (IPA) determination is given in Figure 7. A low atomic number element such as hydrogen produces very strong Compton scattering. The calibration curve was linear for the range of hydrogen

as hydrogen produces very strong Compton scattering. The calibration curve was linear for the range of hydrogen concentrations studied. The relative standard deviation was found to be 2%, which yields a relative error in the hydrogen determination of $\pm 0.15\%$.

Alloy Identification

XRS can also be effective in the identification of alloys containing low Z elements. An aluminum alloy was analyzed by EDXRF and XRS. The EDXRF analysis shows aluminum as the only detectable heavy element. The XRS routine measured an atomic scatter factor of 12.46, and it is known without using the ASF identification algorithm that the ASF of pure aluminum is 13.0. The measured ASF of 12.46 is obviously lower than that of pure aluminum which indicates the presence of a light element. The XRS analysis for low atomic numbered compounds revealed that the ASF of 12.46 corresponded to the material having a composition of $AlLi_{0.012}$, which corresponds to approximately 5% by weight of lithium in the aluminum.

The sample was presented as a flat sheet, therefore no sample preparation was required. The XRS analysis time was approximately 2 minutes.

DISCUSSION

The determination of light elements by EDXRF analysis is hindered by a number of difficulties. One of which is the fluorescence yield, which for atomic numbers below 16, does not exceed 0.05. When an electron transition fills a vacancy in an inner shell there is a certain probability that the emitted x-ray photon will be absorbed in the atom. That is, the emitted x-ray photon ejects an Auger (secondary) electron in one of the outer shells. Figure 8 shows a plot of fluorescence yield (ω) versus atomic number for K, L, and M x-ray lines. Auger electron production is a process that is competitive with x-ray photon emission. The Auger yield ($1-\omega$) increases with decreasing atomic number. Therefore, Auger analysis seems more promising than x-ray analysis, since the low energy photons can not escape from the sample. Typically, the Auger information comes from a surface layer approximately 10-20 Å in depth. By using the Compton-Rayleigh scatter method with molybdenum k-alpha as primary x-ray radiation, the critical depth can be as high as in 300 microns in an aluminum matrix. This critical depth is more representative of the whole sample, and smaller errors will be found when samples are not perfectly homogenous.

CONCLUSION

X-ray scatter spectroscopy has considerable usage for the detection and analysis of low atomic numbered elements from hydrogen to sodium. This technique can provide results that are comparable to conventional infrared and inductively coupled plasma analysis methods.

Covering a wide range of applications, XRS spectroscopy can be used in microelectronics and other contamination control industries; in disciplines involving natural compounds, such as geology, mineralogy, archaeology, and biology; in industries using microstructure composites; in art and artifacts fields for authentication purposes; in material verification; and in environmental problem solving and failure analysis. Obtaining both, XRS and EDXRF information from a single sample will allow the instrument to provide simultaneous chemical and mineralogical data that could be used to characterize unknown materials. Utilization of this information would be indispensable for applications in space exploration such as future missions to the moon and to Mars. This technique can be used for on-stream analysis, continuous control, improved product quality, raw materials savings, and automation of industrial processes.

ACKNOWLEDGEMENTS

The author wishes to extend appreciation to Lore' M. Gandy for her editorial assistance and critical review of this paper. Appreciation is also extended to Chris M. Bourgeois for preparing the samples and for data analysis support.

REFERENCES

- (1) D. E. Leyden, *Fundamentals of X-Ray Spectrometry as Applied to Energy Dispersive Techniques* (Tracor X-ray, Mountain View, California, 1984).
- (2) T. B. Johansson, R. E. Van Greiken, J. W. Nelson, and J. W. Winchester, *Anal. Chem.* **47**, 854-860 (1975).
- (3) E. P. Bertin, *Principles and Practice of X-Ray Spectrometric Analysis* (2nd Ed., Plenum Publishing Corp., N. Y., New York, 1975).
- (4) D. E. Leyden, "Energy Dispersive X-Ray Spectrometry", *Spectroscopy* **2**, 28-36, 1988).
- (5) K. K. Nielson, "Application of Direct Peak Analysis to Energy Dispersive X-Ray Fluorescence Spectra", *X-Ray Spectrometry* **7**, 15-22 (1978).

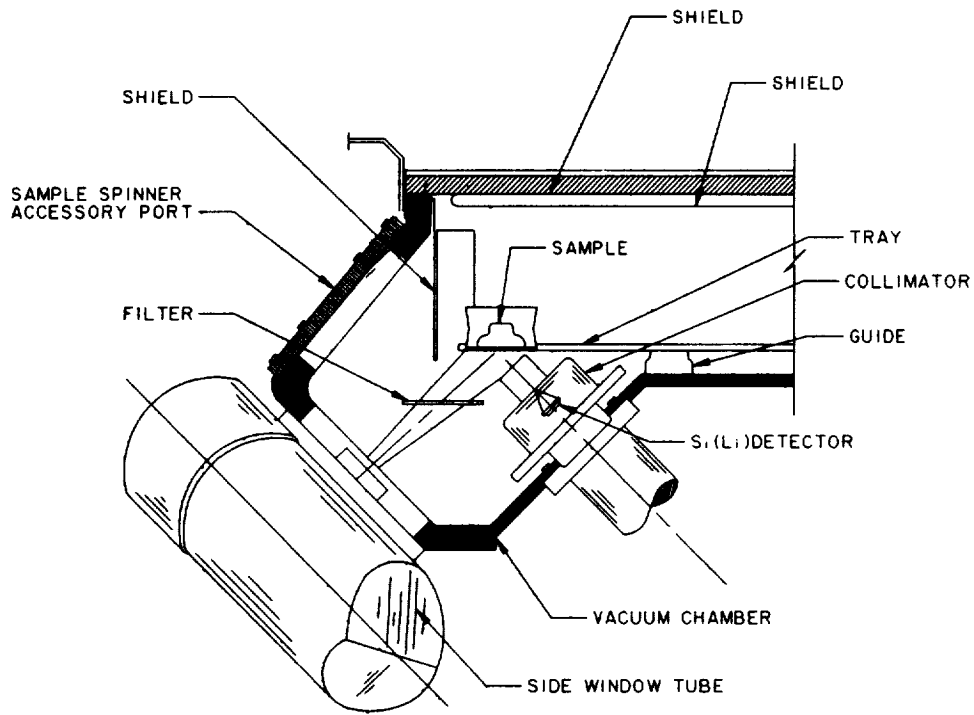


Figure 1: EDXRF System

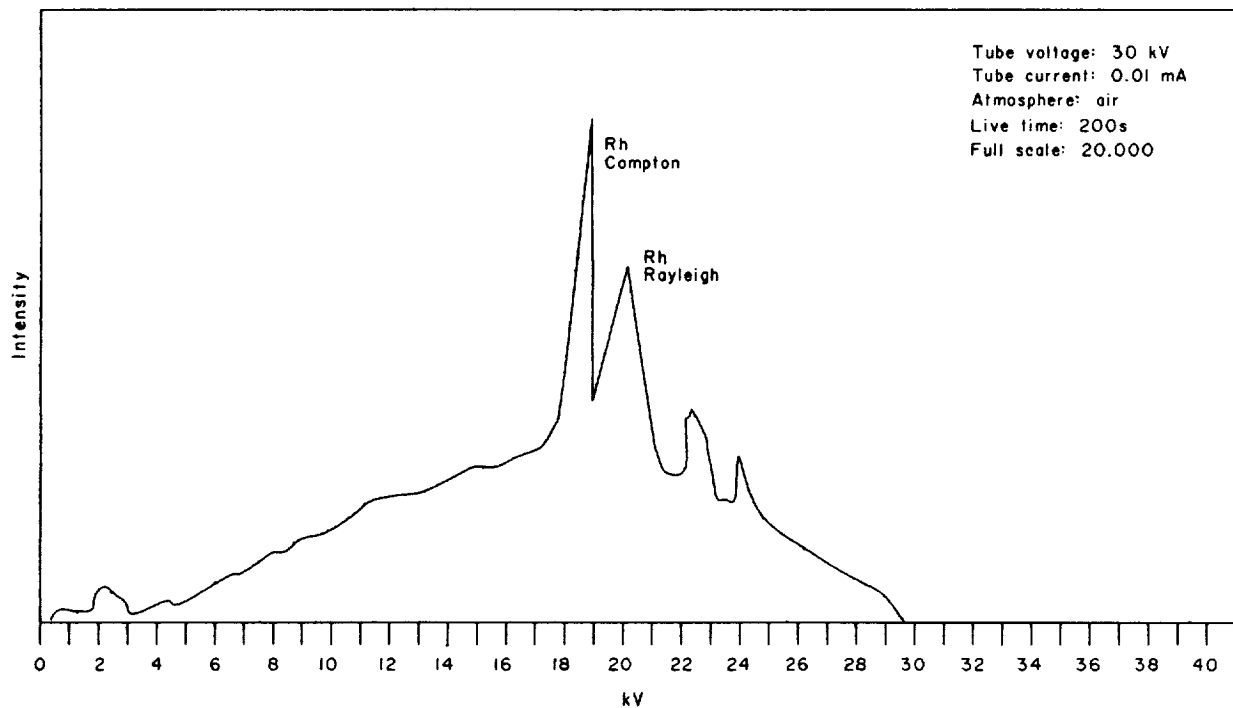


Figure 2: Output of a Rhodium x-ray tube operated at 30 kV scattered from a polyester plug.

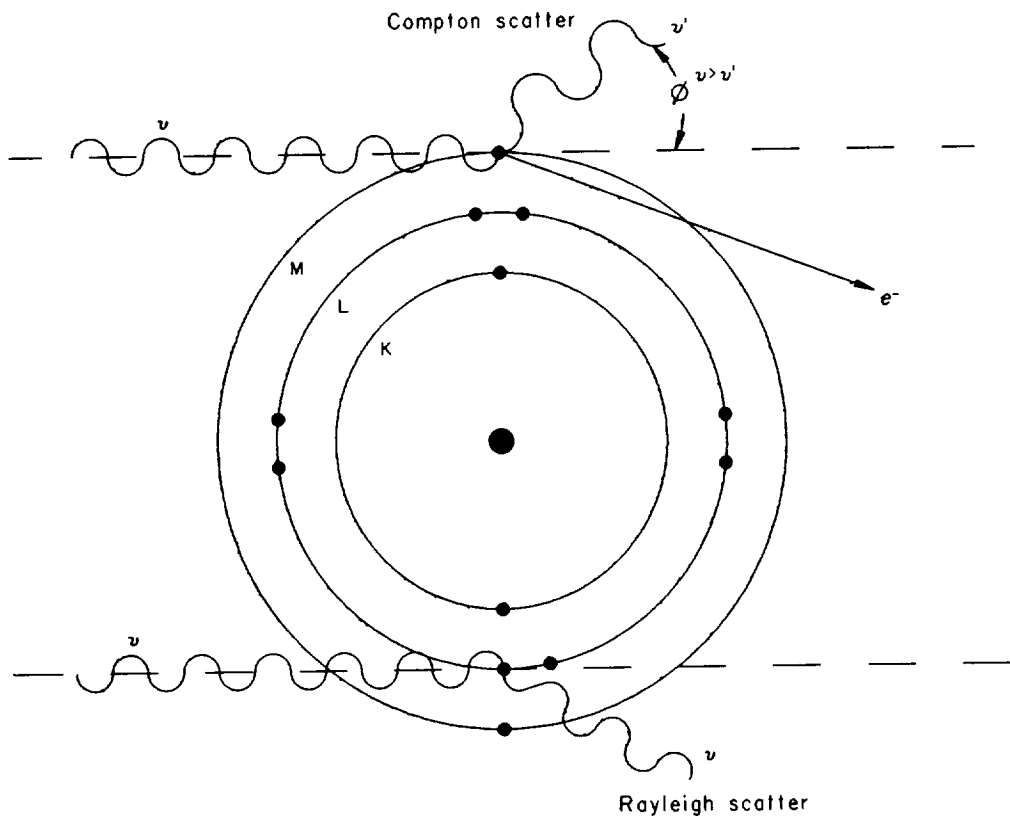


Figure 3: Illustration of Compton and Rayleigh scatter.

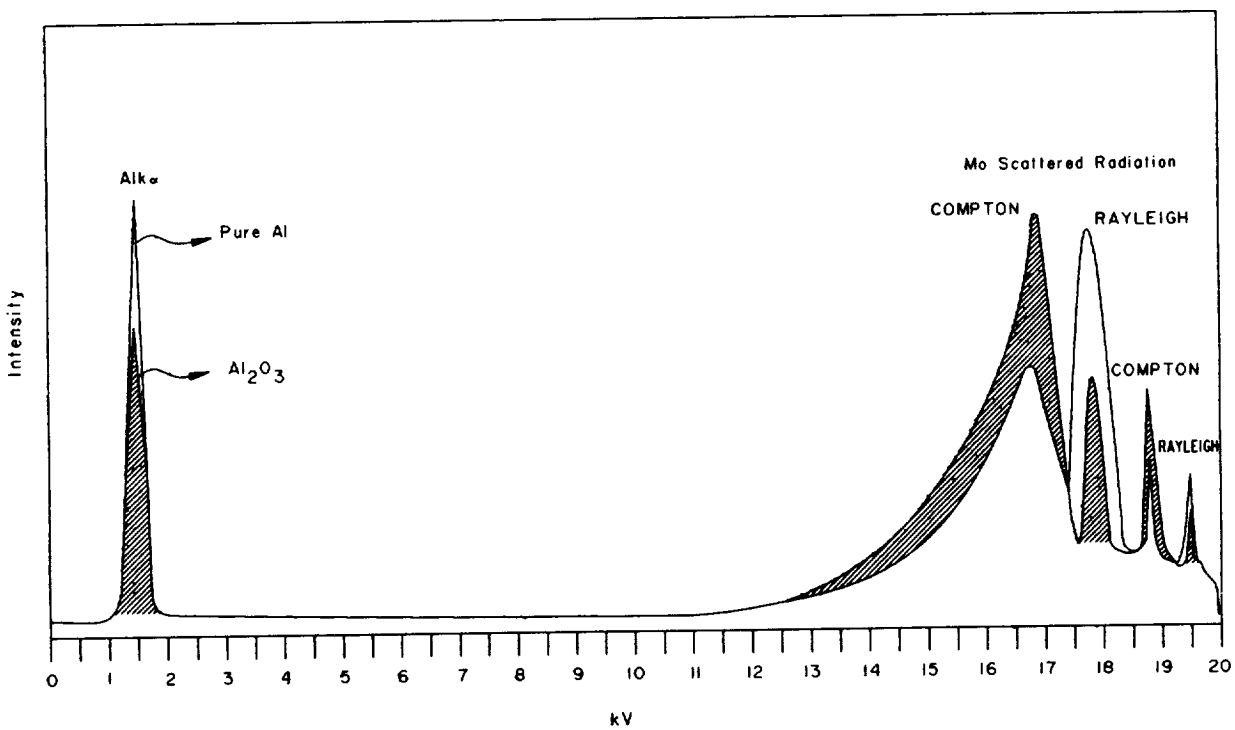


Figure 4: Partitioning of Scatter Intensities - The difference between the light element contributions (shaded area) and heavy element contributions (unshaded areas).

X-RAY SCATTER CALIBRATION CURVE
FOR IRON CONTAINING COMPOUNDS

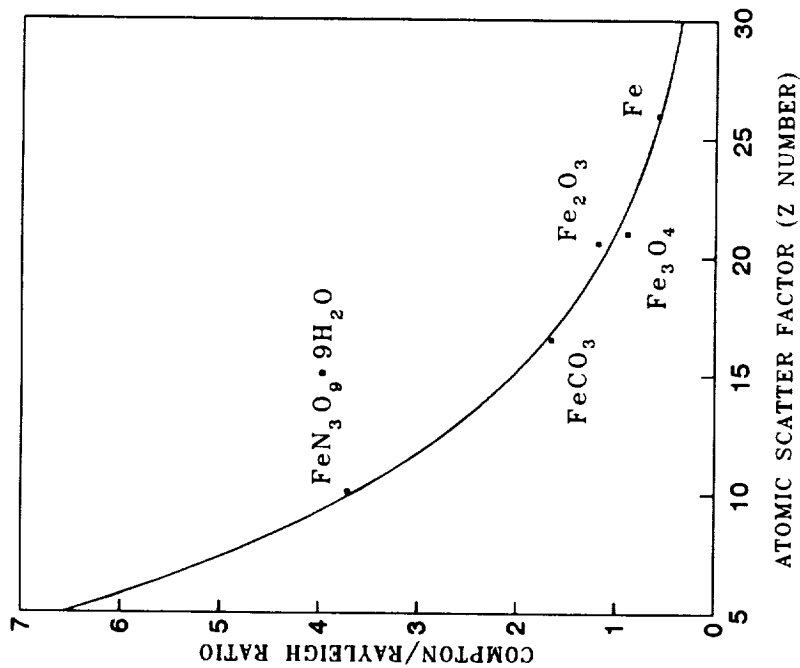


Figure 5: The calibration curve of the x-ray scatter algorithm, relating the Compton/Rayleigh scatter ratio to the ASF. The XRS measures undetected light elements in the sample matrix.

COMPTON RAYLEIGH SCATTER INTENSITIES

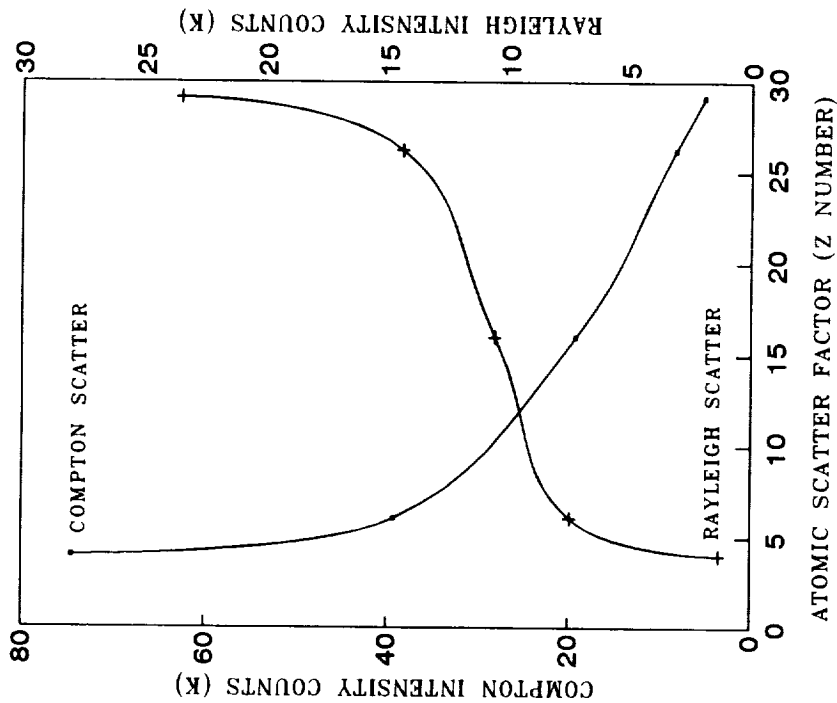


Figure 6: Molybdenum excitation at (50kV) as a function of sample atomic number. The Compton/Rayleigh signals are used to estimate the light element contribution to the total sample matrix.

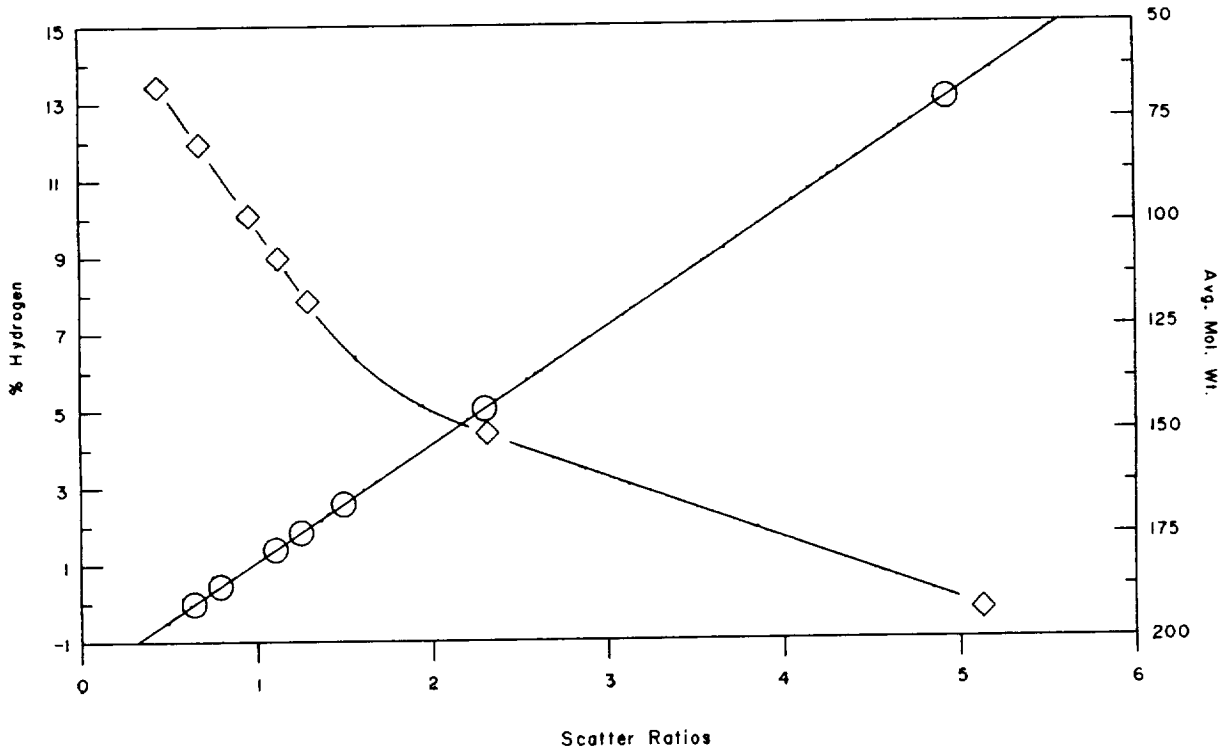


Figure 7: Scatter Ratios vs IPA/CFC 113 Mixtures.

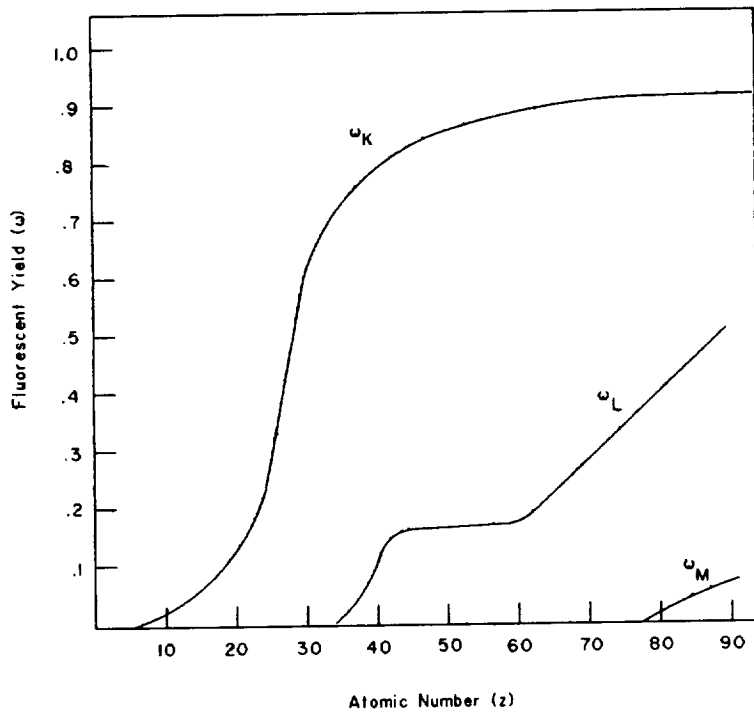


Figure 8: Variation in Fluorescent Yield with Atomic Number.

